PRACTICAL SUPERCONDUCTOR DEVELOPMENT

FOR ELECTRICAL POWER APPLICATIONS

ARGONNE NATIONAL LABORATORY

QUARTERLY REPORT FOR THE PERIOD ENDING DECEMBER 31, 2002

This is a multiyear experimental research program that focuses on improving relevant material properties of high-T_C superconductors and developing fabrication methods that can be transferred to industry for production of commercial conductors. The development of teaming relationships through agreements with industrial partners is a key element of the Argonne National Laboratory(ANL) program.

Technical Highlights

This report summarizes key results from a yearlong effort to apply Raman microscopy methods to the characterization of $MBa_2Cu_3O_x$ (MBCO, where M = Y or a rare earth element) thin films on textured substrates. Important crystallographic features and orientation relationships in coated conductors made by the inclined-substrate deposition (ISD) process are also presented.

Characterization of Coated Conductors by Raman Microscopy

Over the past fiscal year, our investigations of phase composition, cation disorder, and texture quality of coated-conductor embodiments by Raman microscopy methods have been conducted with three objectives in mind: (1) developing an improved understanding of the methodology itself (e.g., in terms of how Raman excitation/configuration parameters influence the observations), (2) investigating systematically prepared groups of samples to provide meaningful correlations with process parameters and with superconductor performance levels (including substantial collaboration with other national laboratories and industrial partners), and (3) examining the applicability of Raman microscopy as an on-line process-monitoring tool during fabrication of long-length coated conductors. A summary of key results from the yearlong effort to characterize $MBa_2Cu_3O_x$ (MBCO, where M = Y or a rare earth element) thin films on textured substrates is presented below.

One of the issues involved in interpreting the Raman microscopy results has been the matter of laser penetration depth, i.e., what portion of the sample is being interrogated. Figure 1 shows the results of Raman microprobe measurements on three EuBCO films of varying thickness deposited by pulsed laser deposition (PLD) on La-Sr-Al-Ta-O (LSAT) substrates. This series of samples, prepared by Q. Jia at Los Alamos National Laboratory (LANL), consisted of uniformly deposited EuBCO films, free of cracks, voids, and other imperfections that might allow the laser to strike bare substrate.

Employing a 633-nm laser excitation wavelength at a surface power density of ≈0.2 mW per μm^2, and using the LSAT phonon at ≈470 cm^{-1} as a guide, we found (see Fig. 1) that the LSAT was readily detectable at an EuBCO thickness of 0.19 μm, barely detectable at a thickness of 0.3 μm, and undetectable at a thickness of 0.5 μm. We have concluded from this study that for the excitation conditions we typically use to investigate MBCO films, the depth below the MBCO surface from which detectable Raman scattering emanates is approximately 0.3 μm.

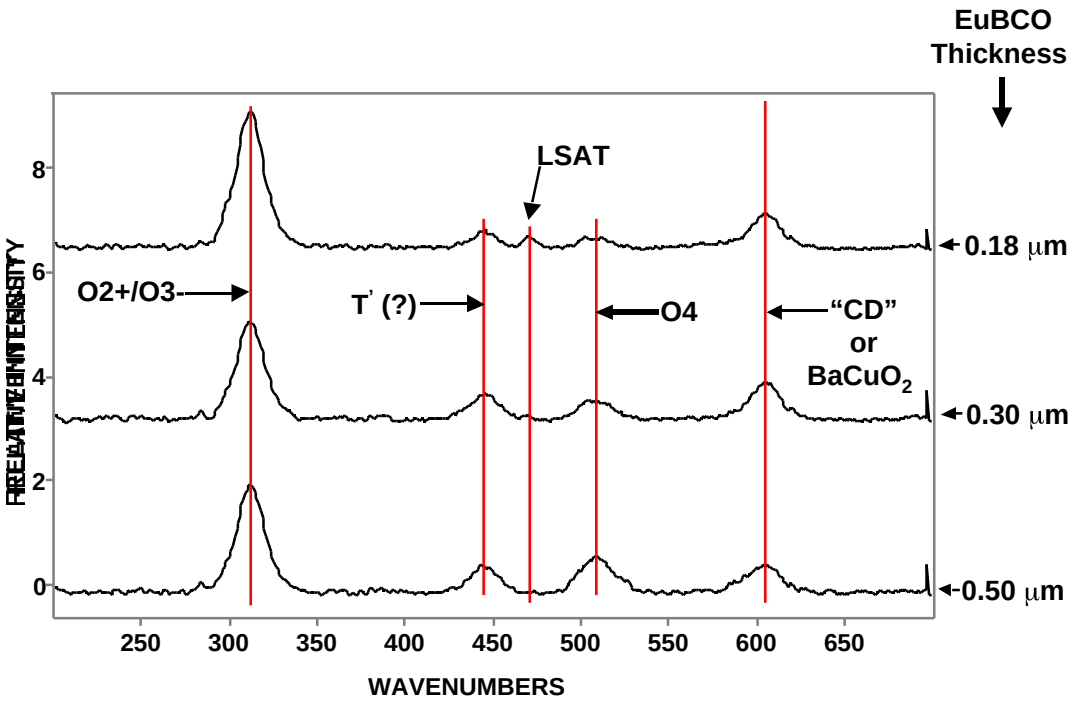

Fig. 1. Raman microprobe spectra for three thicknesses of PLD-type EuBCO on single-crystal La-Sr-Al-Ta-O (LSAT) substrates. "CD" represents cation disorder.

It will be useful in the further reading of this summary to note that most of the informative features in typical Raman spectra of the MBCO films we have studied thus far appear in Fig. 1. These features include (1) the O2+/O3- and O4 phonons of orthorhombic MBCO, the relative intensities of which provide information about the c-axis tilt associated with the presence of "a-axis" grains or tilted MBCO grains (as discussed in previous quarterly reports), (2) modes that are associated with cation disorder and/or the presence of barium cuprate second phases, and (3) the mode at ≈450 cm^{-1}, which indicates the presence of residual tetragonal MBCO domains.

Figure 2 shows the results of a study conducted to investigate the influence of laser excitation wavelength on the observed Raman spectra of YBCO films of varying thickness. These samples, from a series of specimens provided by A. Goyal of

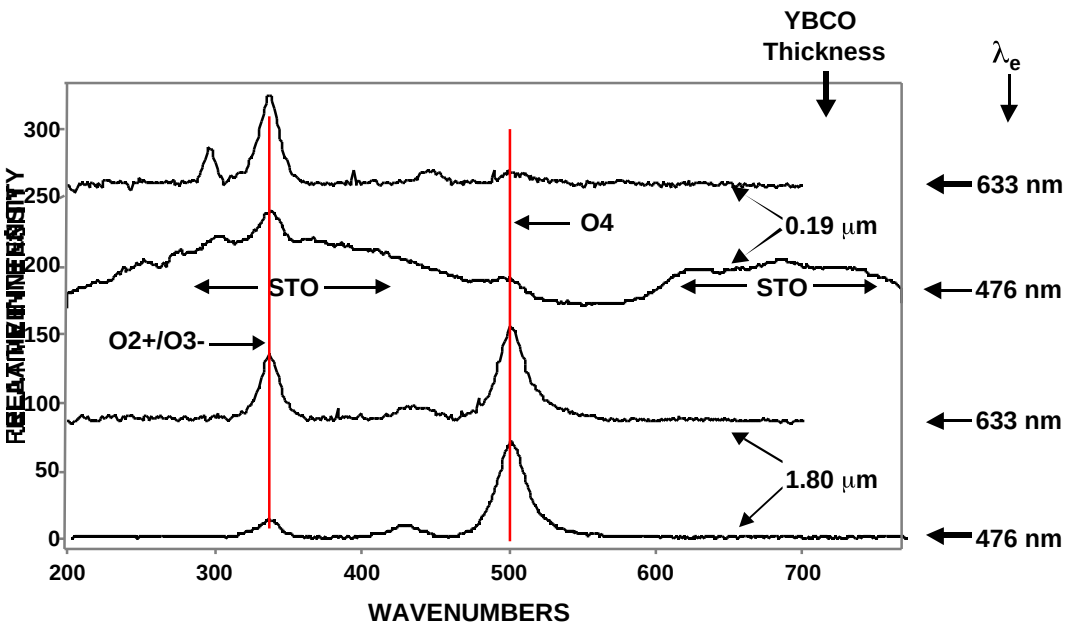

Fig. 2. Raman spectra of 0.19- and 1.80-μm-thick PLD-type YBCO films on single-crystal $SrTiO_3$ (STO) recorded with two laser excitation wavelengths (λ_e = 633 and 476 nm).

Oak Ridge National Laboratory (ORNL), consist of PLD YBCO on single-crystal $SrTiO_3$ (STO). The spectrum of the 0.19-μm-thick film, taken with 476-nm excitation, exhibits broad underlying background features centered near 330 cm^{-1} and 700 cm^{-1} that are due to resonance enhancement of the second-order Raman spectrum of STO. Note that this enhancement is not seen with 633-nm excitation. For the thicker YBCO specimen, the spectra obtained with 633- and 476-nm excitation are qualitatively similar in terms of the observed spectral features and the signal-to-noise level. The reduced intensity of the O2+/O3- mode relative to the O4 mode with 476-nm excitation is attributed to less penetration of the YBCO when compared with the case for 633-nm excitation, and is most probably a consequence of the presence of more "a-axis" YBCO near the surface of the film than in the bulk. In essence, the 633-nm excitation penetrates deeper into the film (where there is less "a-axis" grain development) than does the 476-nm excitation. We find that, in general, 633-nm excitation is superior to 476-nm excitation for measurements on MBCO coated conductors, because it exhibits a lesser tendency to stimulate resonantly enhanced spectra and because it penetrates more deeply into the MBCO film. Similar comparative studies with 514-nm excitation revealed that laser wavelengths in the "green" part of the spectrum tend to preferentially excite the resonance enhanced Raman spectra of $BaCuO_2$ without improving the penetrating ability of 633-nm radiation.

Observation over the past year of a band near 450 cm^{-1} in the Raman spectra of YBCO-coated conductor specimens from several collaborating institutions has prompted us to more thoroughly investigate its origin. To confirm our initial presumption that this mode is due to tetragonal YBCO domains within largely orthorhombic YBCO thin films (a circumstance commonly referred to as phase separation in connection with YBCO phase evolution), we examined several samples that contained this mode as a prominent spectral feature (samples provided by S. Foltyn at LANL). In Fig. 3, we show spectra of two of these samples, both PLD YBCO on a buffered metal substrate (in one case IBAD YSZ / Hastelloy C, in the other, a Ni-RABiTS substrate provided by ORNL), together with the spectrum of a melt-processed YBCO sample known to be tetragonal YBCO (obtained from P. Diko at the Slovak Academy of Sciences). This observation calls attention to the possibility that oxygenation of YBCO films may, in some cases, be either incomplete or somehow inhibited during fabrication of coated conductor specimens. The extent to which this phase separation acts to degrade critical current density (J_c) and / or contributes in a beneficial way to flux pinning remains to be determined.

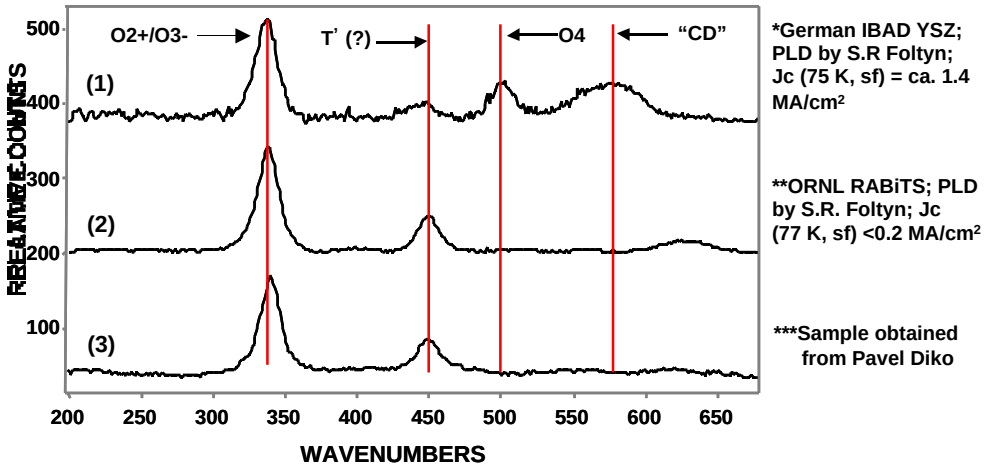

Fig. 3. Raman microprobe spectra of YBCO samples exhibiting the 470 cm^{-1} mode indicative of tetragonal form of YBCO: (1) YBCO (1.2 μm by PLD) / SmBCO (0.1 μm by PLD) / YBCO (1.2 μm by PLD) / CeO_2 / YSZ / Hastelloy C,* (2) YBCO (1.0 μm by PLD) / CeO_2 / YSZ / CeO_2 / Ni-RABiTS,** (3) tetragonal YBCO bulk specimen (melt-processed / textured).*** See notes in figure for additional details.

In collaboration with A. Goyal at ORNL, we performed Raman measurements on a series of PLD YBCO films of varying thickness deposited on STO to investigate changes in film composition and c-axis alignment as YBCO film thickness increased. The results of this study, shown in Fig. 4, indicate that the onset of tilted YBCO grain growth begins to occur at thickness values between 0.4 and 0.7 μm. (This is determined by the increase

in intensity of the O4 mode of YBCO at 500 cm^{-1} relative the O2+ / O3- mode at 340 cm^{-1}.) In Fig. 4, it is noteworthy that the J_c initially drops off with increasing film thickness but eventually reaches a relatively constant value at a YBCO thickness near 0.7 μm. In an independent investigation of these same samples using X-ray scattering methods, Kang et al. [1] also correlated this behavior with the progressive growth of "a-axis" grains within the c-axis films, as well as with a general broadening of the in-plane texture.

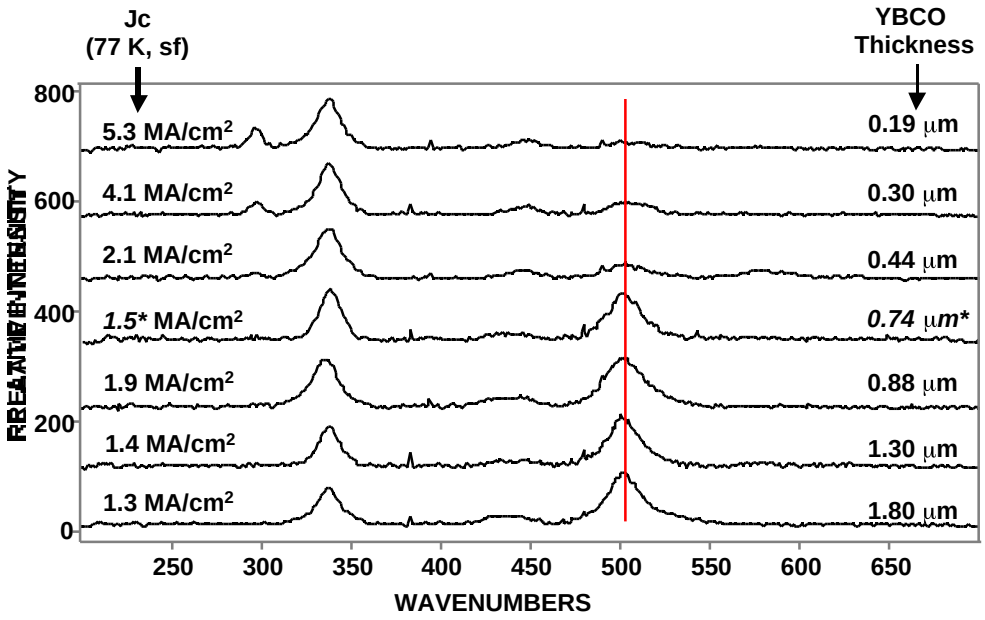

Fig. 4. Averaged Raman microprobe spectra of PLD-type YBCO films of varying thickness. Each plotted spectrum is the average of individual spectra taken at nine locations on specimen surface. Films with thickness = 0.19, 0.30, 0.44, 0.88, 1.30, and 1.80 μm are on single-crystal STO substrates. Film with thickness = 0.74 μm* is on single-crystal $LaAlO_3$.

The effect of "a-axis" grain growth on the texture quality of the YBCO films can be seen in Fig. 5, which shows the results of texture mapping performed with the Raman microprobe. In this mapping procedure, we collect Raman spectra at evenly spaced locations throughout the section of the film lying between the current leads used to measure electrical properties. From these spectra, we obtain values for the intensity (I) of the 500 and 340 cm^{-1} modes of YBCO, calculate the intensity ratio (I_{500}/I_{340}), and use this ratio to create a contour map of the texture profile, as shown in Fig. 5. An increasing value of I_{500}/I_{340} implies increasing "a-axis" grain presence. From the results in Fig. 5, it is clear that the through-thickness texture (assuming full penetration by the laser) of the thinner YBCO film (0.19 μm) is much better than that of the outer ≈0.3 μm layer of the thicker (1.8 μm) film.

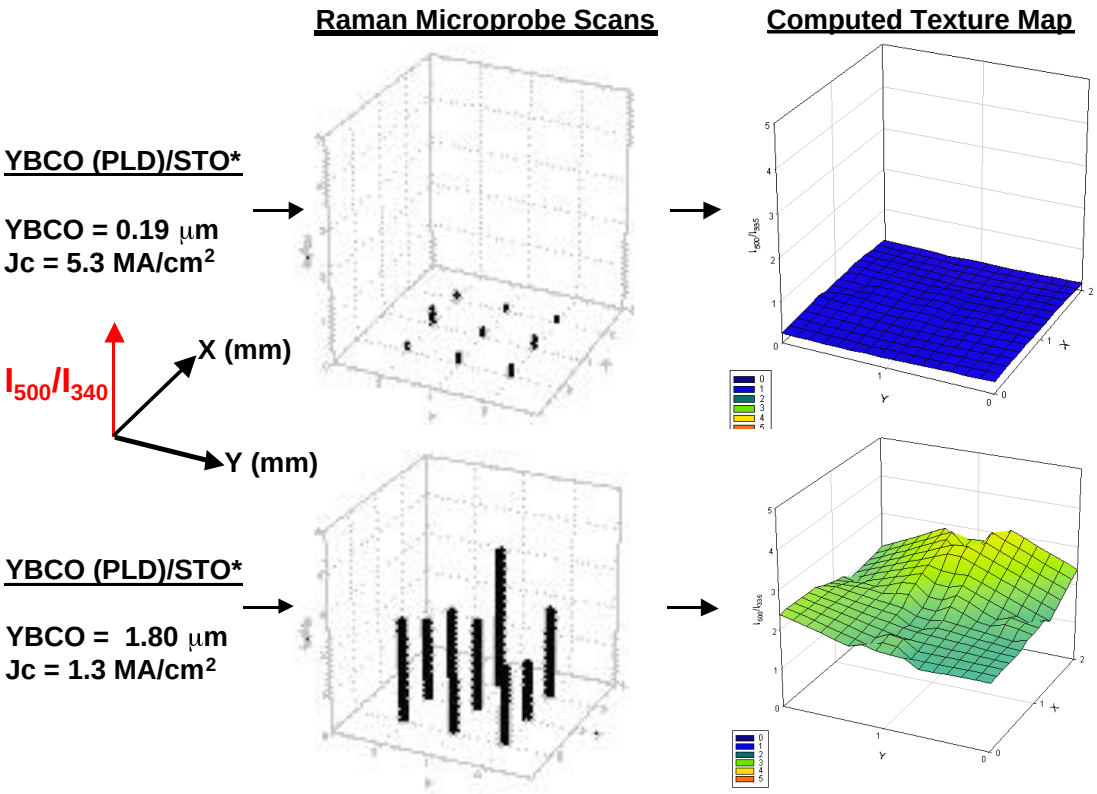

Fig. 5. Results of Raman microprobe texture mapping for 0.19- and 1.80-μm-thick PLD-type YBCO films on single crystal $SrTiO_3$ (STO). Poles in scan plots indicate spatial locations and corresponding I_{500}/I_{340} values. Texture maps show computer-generated textured maps based on I_{500}/I_{340} values in scan plots.

In collaboration with R. Feenstra at ORNL, we have begun an investigation of the composition and texture quality of ex situ-type YBCO films produced by the BaF_2 process. The J_c values of ex situ YBCO films on buffered metal substrates are comparable to those of PLD films on the same substrate systems. Raman microprobe spectra for ex situ YBCO films of varying thickness deposited on LANL-produced CeO_2/IBAD YSZ/Ni-alloy and ORNL-produced CeO_2/YSZ/Y_2O_3/Ni-RABiTS substrates are shown in Fig. 6, together with the YBCO thickness and J_c value for each specimen. From these studies, we find that the ex situ films contain a relatively small but measurable fraction of tilted YBCO grains due either to general topographic roughness or "a-axis" grain clusters. This can be seen in Figure 6 by comparing the relative intensities of the O4 and O2+/O3- phonons (i.e., I_{500}/I_{340}). Whereas "a-axis" grain growth exhibits an onset thickness for PLD-type YBCO films, as discussed above for the results in Fig. 4, "a-axis" grains seem to form in a thickness-independent manner for the ex situ-type of YBCO film, i.e., they persist in small quantity throughout the film as opposed to increasing in amount with increasing film thickness.

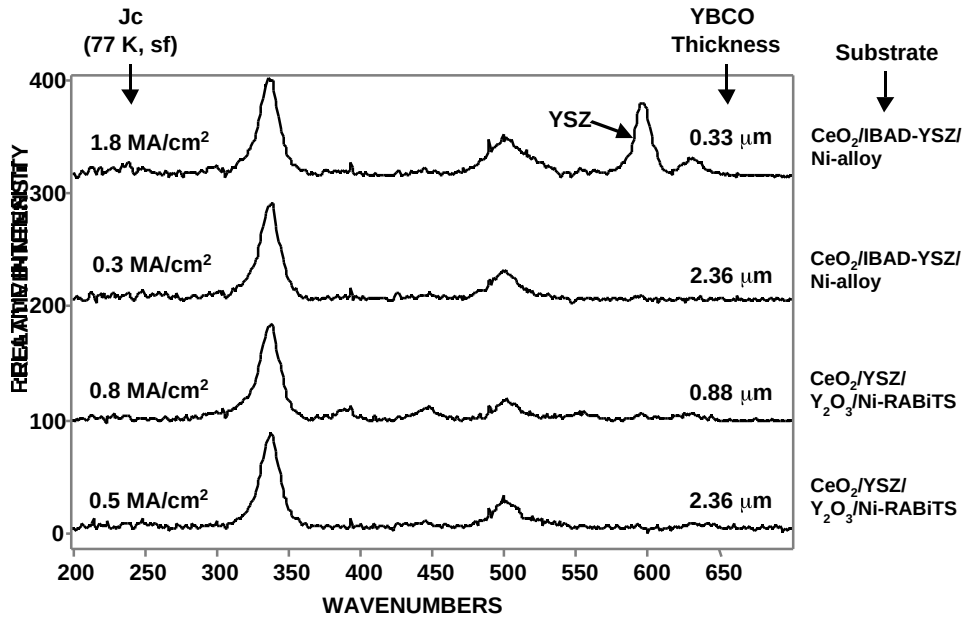

Fig. 6. Raman microprobe spectra of YBCO films produced by BaF_2-type ex situ process. Information on type of substrate, film thickness, and measured J_c is given for each film. IBAD substrates were produced at LANL; RABiTS substrates, at ORNL; films were deposited by R. Feenstra et al. at ORNL.

Figure 7 shows the Raman-generated texture maps for the four samples in Fig. 6, together with a graph of J_c vs. YBCO thickness for various ex situ YBCO-coated conductor embodiments supplied by Feenstra et al. of ORNL. The quality / uniformity of the texture, which is reasonably good but not perfect, is comparable for all four samples. This finding seems to be relatively independent of substrate type, at least for the four samples we examined. From inspection of the data points in the inserted graph in Fig. 7, one can deduce that the dependence of J_c on film thickness (t) for ex situ YBCO generally conforms to a simple relationship of the form $\log(J_c)$ -log(t).

During the past year, we have been using Raman microscopy to monitor phase evolution and texture quality in connection with the deposition of YBCO (by PLD) on rolled Ag and Ag alloy substrates. Several informative correlations have been developed between film J_c and process-related parameters. We found that adding a small percentage of Cu to the Ag improved J_c values and that there appeared to be an optimum value for the Cu content. Figure 8a shows Raman spectra of four YBCO films on Cu-Ag alloy substrates with a range of Cu contents. The critical temperature (T_c) and magnetization-derived driving current measured for each of these four YBCO films is plotted in Fig. 8b. The value of I_{500} / I_{340} for each sample (also plotted Fig. 8b) reaches a minimum at Ag-0.2 at.% Cu, which correlates with that specimen being the best performer in the group. Based on the criteria for texture quality discussed above (i.e.,

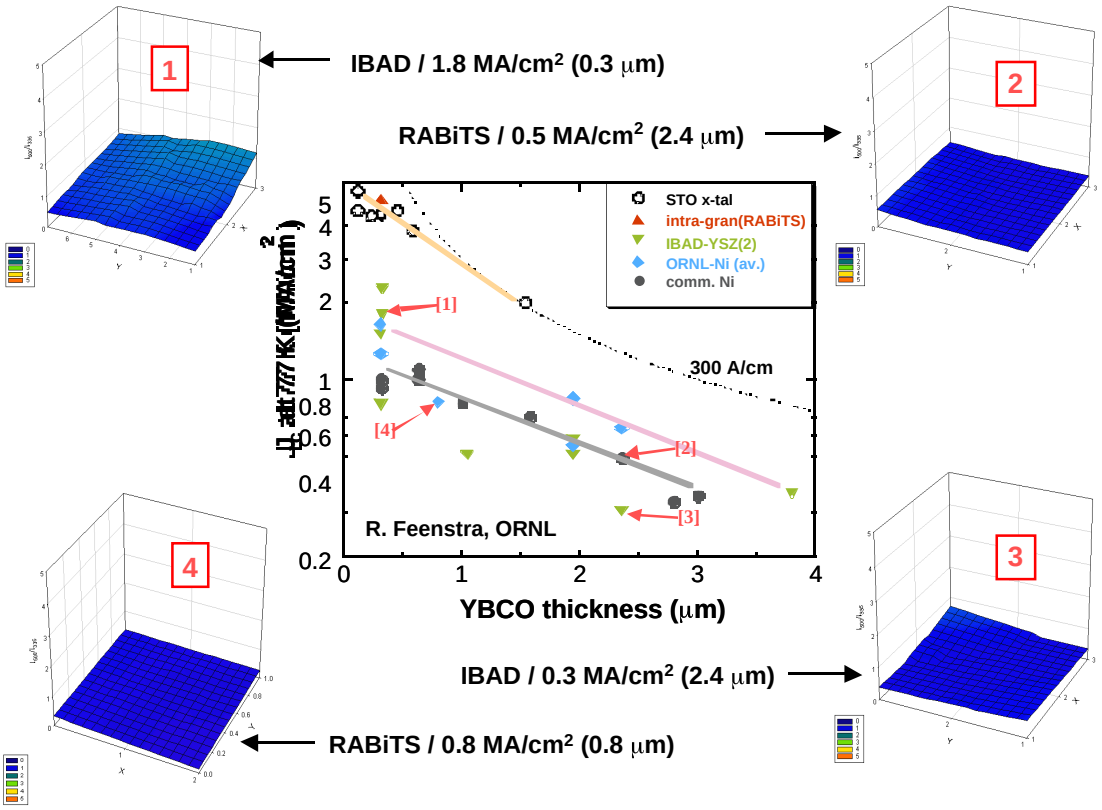

Fig. 7. Texture maps generated by Raman microprobe data for the four samples in Fig. 6. Graph shows J_c vs. YBCO thickness for the four samples, together with values for other ex situ YBCO films on various types of substrates.

$I_{500}/I_{340} \rightarrow 0$), it is clear that the YBCO film on Ag-0.2 at.% Cu exhibits the least evidence of tilted YBCO grains and no evidence of cation disorder (≈580 cm^{-1}) or second phases. A related study of the effect of laser pulse energy density on the performance of the deposited YBCO film produced a similar correlation with texture quality. I_{500}/I_{340} values obtained from the Raman spectra presented in Fig. 9a reached a minimum at the same energy density (138 mJ/cm^2) that yielded the best performing YBCO / Ag-0.2 at.% Cu specimen, as shown in Fig. 9b. Also, the Raman spectrum of the sample deposited at a 130-mJ/cm^2 pulse energy exhibited evidence of cation disorder (≈580 cm^{-1} in Fig. 9a), which may be related to the observation that the driving current for this sample was lower than expected, based on the trend in driving current values evident in Fig. 9b. This observation adds to the mounting evidence in our Raman studies of YBCO-coated conductors indicating that cation disorder is detrimental to performance.

One of the objectives of our Raman microprobe investigations has been to develop Raman-based methods for conducting on-line monitoring of long-length coated conductor manufacturing processes. A test study was conducted in collaboration with

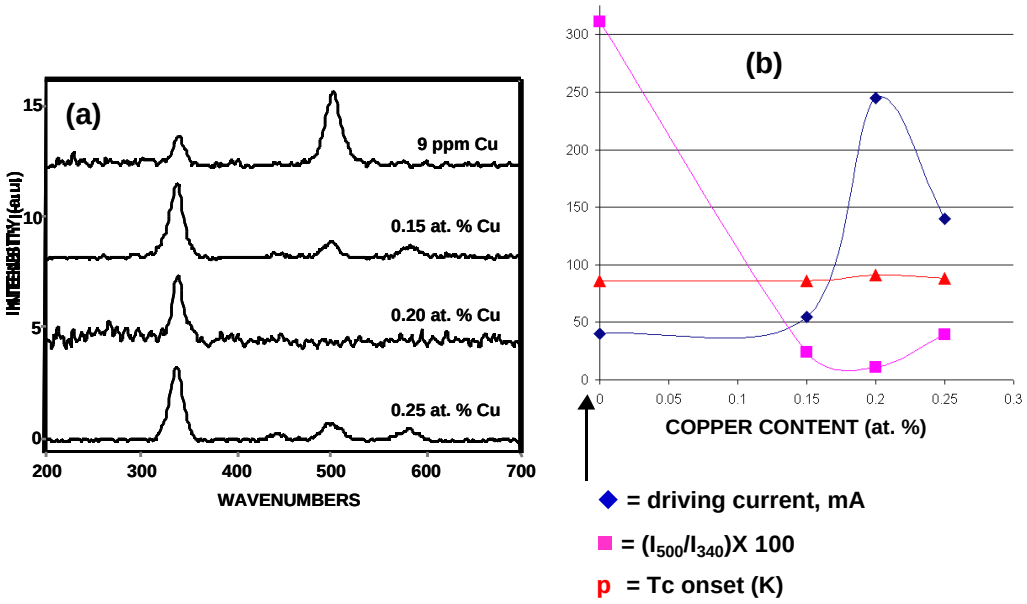

Fig. 8. (a) Raman microprobe spectra for PLD-type YBCO on roll-textured Ag-Cu substrates with varying Cu content. (b) Combined plot of magnetization-based driving current (as a J_c metric), I_{500}/I_{340} value obtained from Raman spectra, and T_c value for each YBCO film reported in (a) as a function of Cu content of substrate.

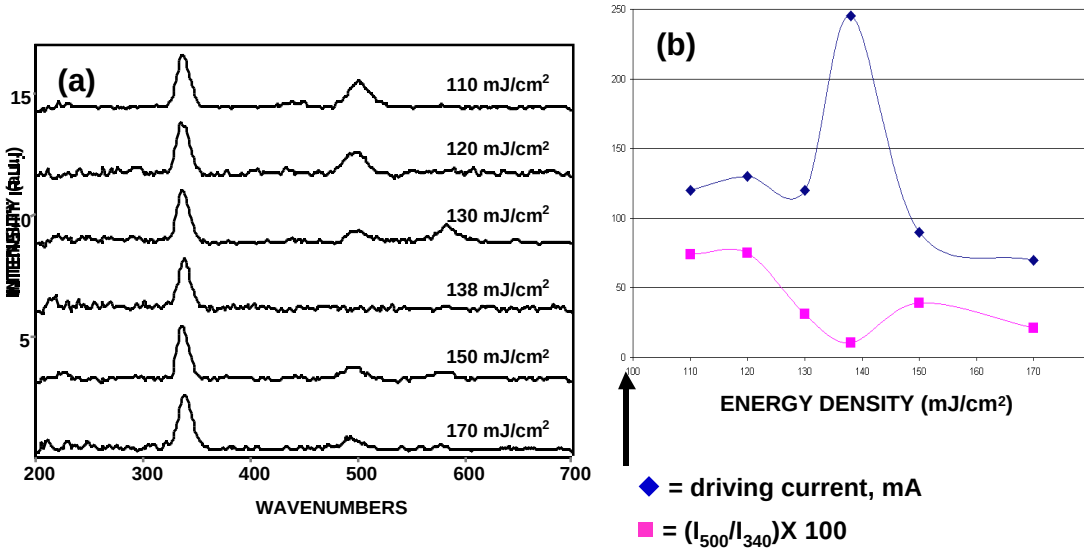

Fig. 9. (a) Raman microprobe spectra of PLD-type YBCO on Ag-0.2 at.% Cu substrates deposited at differing laser pulse energy densities. (b) Combined plot of magnetization-based driving current (as a J_c metric), and I_{500}/I_{340} value obtained from the Raman spectra in (a) as a function of laser pulse energy density.

ChemIcon, Inc. (Pittsburgh, PA) to gauge focal-length requirements for sufficiently sensitive detection of YBCO phonons. Figure 10 summarizes results of Raman microprobe measurements that were performed on a YBCO / CeO_2 / Hastelloy-C specimen for a range of objective magnifications and working. These results indicate that the O2+ / O3- (≈340 cm^{-1}) and O4 (≈500 cm^{-1}) modes of YBCO can be detected with useful sensitivity out to a working distance of 21 mm. The Raman spectra in Fig. 10 were excited with a laser wavelength in the "green" portion of the visible spectrum, hence, the characteristic $BaCuO_2$ mode (≈640 cm^{-1}) is sufficiently enhanced that it is still noticeable out to the longest working distance (21 mm). Even the tetragonal YBCO mode at ≈450 cm^{-1} and the cation disorder mode at ≈580 cm^{-1} are discernable out to a working distance of nearly 10 mm. These results provide encouraging evidence that Raman-based diagnostics could be used effectively to monitor phase evolution during YBCO-coated-conductor processing. At ambient temperature, the working distance

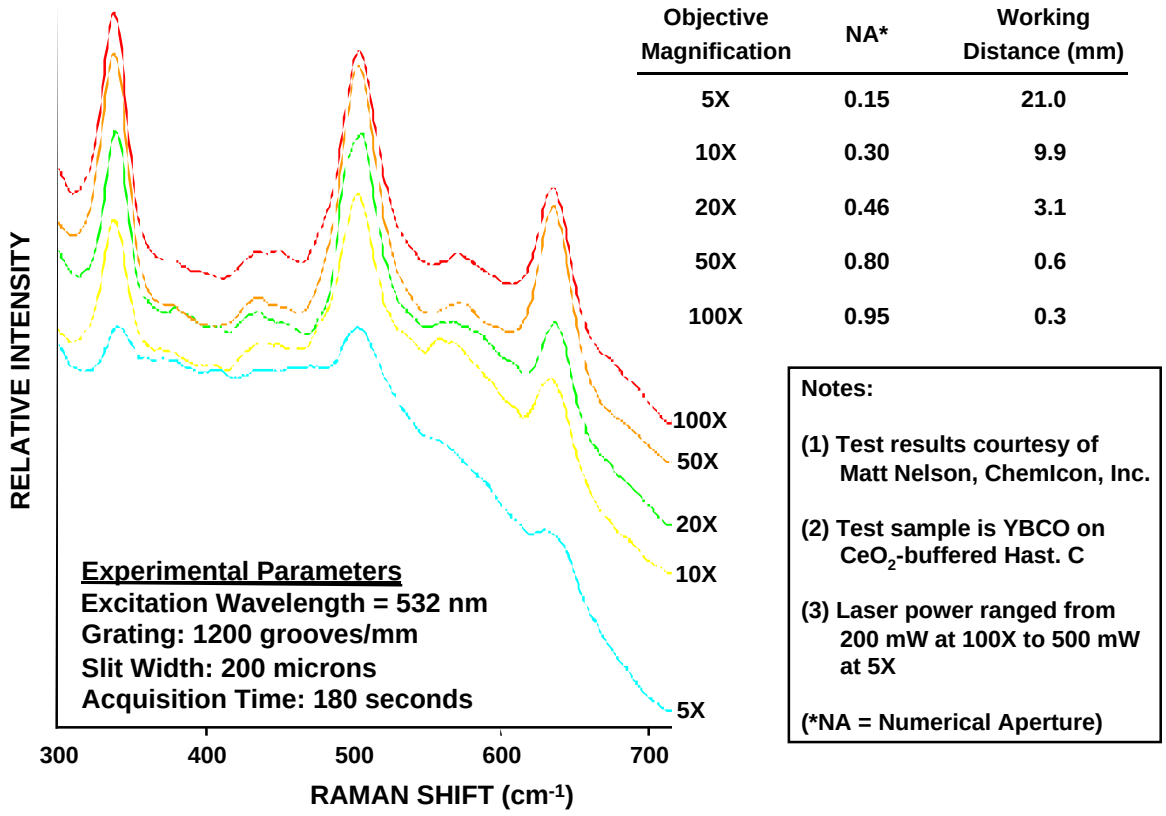

Fig. 10. Results of Raman microprobe measurements on YBCO-coated-conductor specimen as a function of objective magnification, numerical aperture (NA), and working distance.

could easily be as small as 0.5 mm without disturbing the surface of a moving tape. In elevated-temperature environments (even up to 800°C), it should be possible to design/construct actively cooled optical bayonets that accommodate the taking of Raman spectra at working distances on the order of 20 mm.

Texture Development and Crystallography of ISD-based Coated Conductors

Inclined-substrate deposition is an approach for synthesis of biaxially textured templates that is complementary to IBAD and RABiTS. ISD is a simple, fast process that has been demonstrated to grow highly textured MgO. The texture development is independent of substrate, occurs at room temperature, and is highly amenable to scale-up. Studies have been carried in the Electron Microscopy Center at ANL to elucidate the texture formation mechanism, establish the microstructure of the textured template and subsequent layers, and identify the crystallography and orientation relationships between each layer.

Figure 11 shows a series of electron diffraction patterns from the ISD MgO template as a function of thickness. The broadening of the fundamental reflections is a measure of the range of grain orientations within the selected area. By measuring the angular width of the reflection, the texture can be determined as a function of thickness (equivalent to time), as shown in Fig. 12.

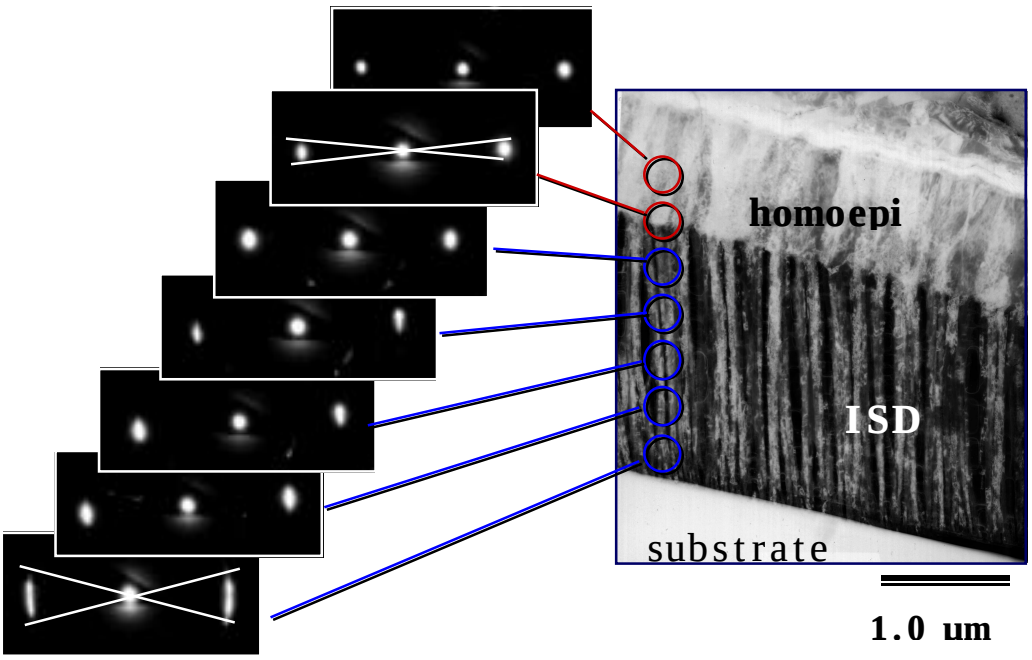

Fig. 11. Electron diffraction patterns from various points through the thickness of ISD-MgO template. Width of reflection indicates sharpness of texture.

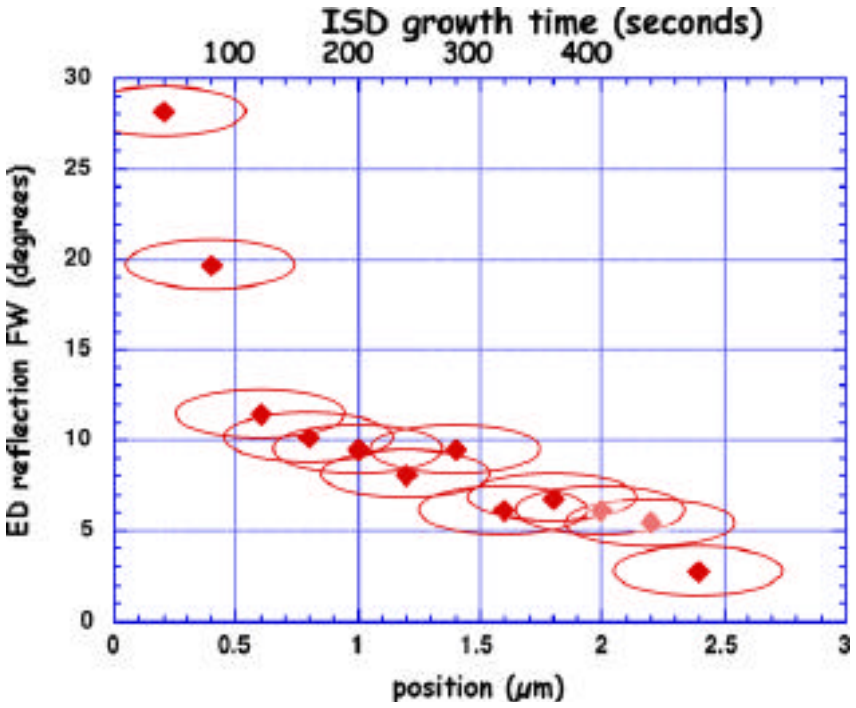

Fig. 12. Texture (as measured by full-width of electron diffraction reflection) through thickness of an ISD-MgO template. Lighter-shaded points (2.0-2.2 μm) were measured from an area that included both ISD and homoepi MgO; points to the left were measured from ISD MgO only, and point to the right from homoepi MgO only.

The plot of texture (as measured by the full-width of electron diffraction reflection) as a function of thickness (Fig. 12) reveals two notable features. First, a high degree of texture develops very rapidly, reaching a plateau-like value at a thickness of ≈0.5 μm (a growth time of ≈2 min for these deposition conditions). Second, addition of the homoepitaxial cap layer further improves the texture. The improvement in texture due to the cap layer has been confirmed by similar measurements on ISD films of differing thickness. In each case, the homoepitaxial cap layer yields an improvement in texture.

The rapid development of texture is significant in terms of the efficiency of the ISD process. The further evolution of texture during growth of the epitaxial cap layer is shown in Fig. 13, where a single grain in the homoepitaxial layer caps three ISD grains in the two-dimensional plane of the image; considering the dimension out of this plane, such grains appear to cap on the order of 10 ISD grains. The improvement in texture occurs because the homoepitaxial grains eventually adopt “mid-range” orientations.

Figure 14 shows a bright-field transmission electron microscopy (TEM) image and corresponding electron diffraction pattern for a coated-conductor architecture that is based on ISD. In the image, the homoepitaxial MgO, YSZ, Ce-containing layer, and the

YBCO layer are each visible. The selected area diffraction pattern shows reflections from each of these layers, from which the orientation relationships can be established. In this particular case, the ceria has reacted during YBCO growth to form $BaCeO_3$, so the orientation relationship before deposition cannot be determined. However, for each of the other layers, a specific orientation relationship is observed, as shown in Fig. 14. Thus, the epitaxial nature of growth through each of the layers is established.

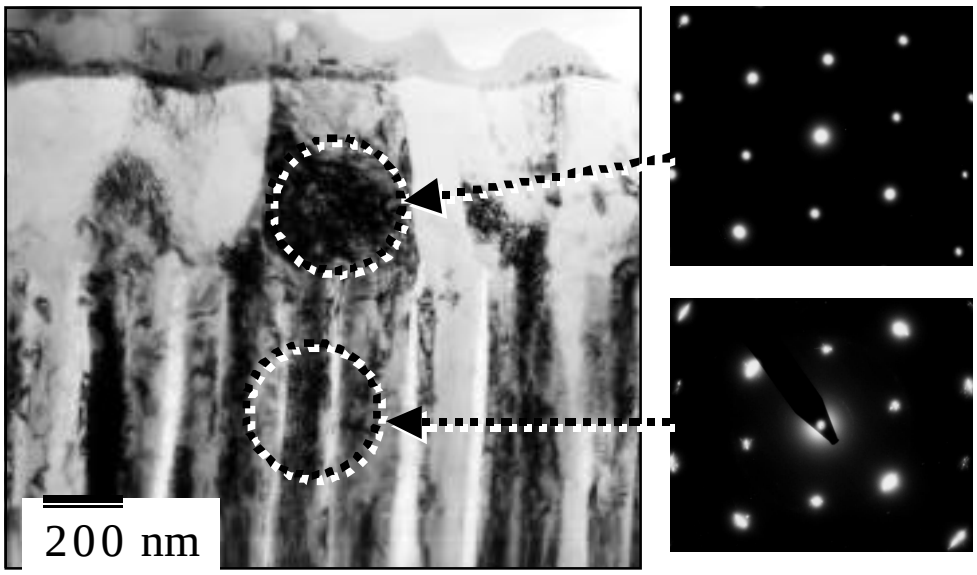

Fig. 13. Electron diffraction patterns from ISD-MgO and homoepitaxial MgO layers showing enhancement of texture by homoepitaxial layer.

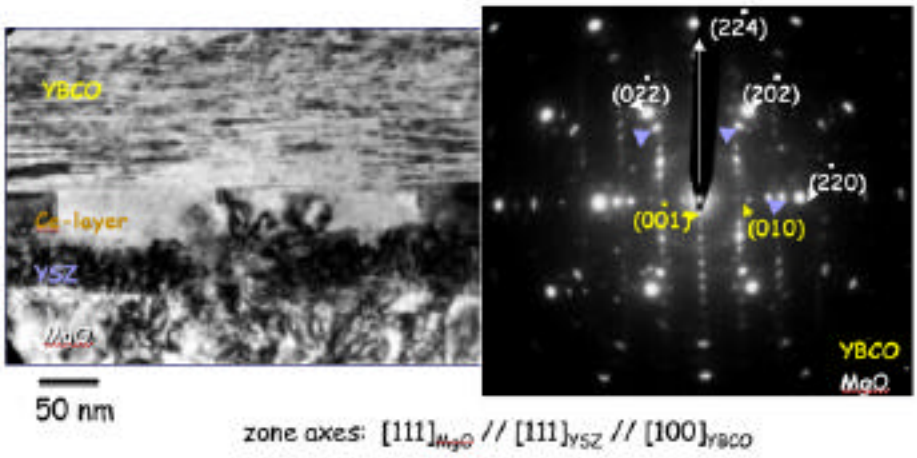

Fig. 14. Bright-field TEM image from ISD-based coated conductor and corresponding electron diffraction pattern used to determine orientation relationships.

An intriguing aspect of ISD-based coated conductors is that YBCO films can be produced with their c-axis normal to the substrate (see Fig. 14), even though the [002] planes of MgO are inclined with respect to the substrate normal. YBCO films with c-axis oriented normal to the substrate offer some advantages over inclined orientations in that significant in-plane anisotropy can be avoided, and most design and modeling is based on films with the c-axis oriented normal to the substrate. The orientation of the YBCO depends on the crystallography of the underlying layers. For growth on some perovskite buffers, direct cube-on-cube epitaxy occurs, leading to an inclined YBCO orientation. However, with the (211) surface plane that is presented by the "inclined" growth of CeO_2 as the top buffer, the situation differs. Because the lattice constants of YBCO and CeO_2 differ, cube-on-cube epitaxy in the inclined orientation leads to a relatively poor match for the YBCO (001) planes. In this situation, it is probable that crystalline anisotropy dictates YBCO growth in a c-axis orientation. Reciprocal space representations of the CeO_2 [211] and YBCO [001] planes are shown in Fig. 15. From these representations, it is evident that one orientation will favor minimization of elastic interactions: CeO_2 (001) // YBCO (010), the orientation relationship that is observed experimentally. Thus, YBCO that is deposited onto these ISD-based templates exhibits a high degree of texture that is dictated by the underlying layers.

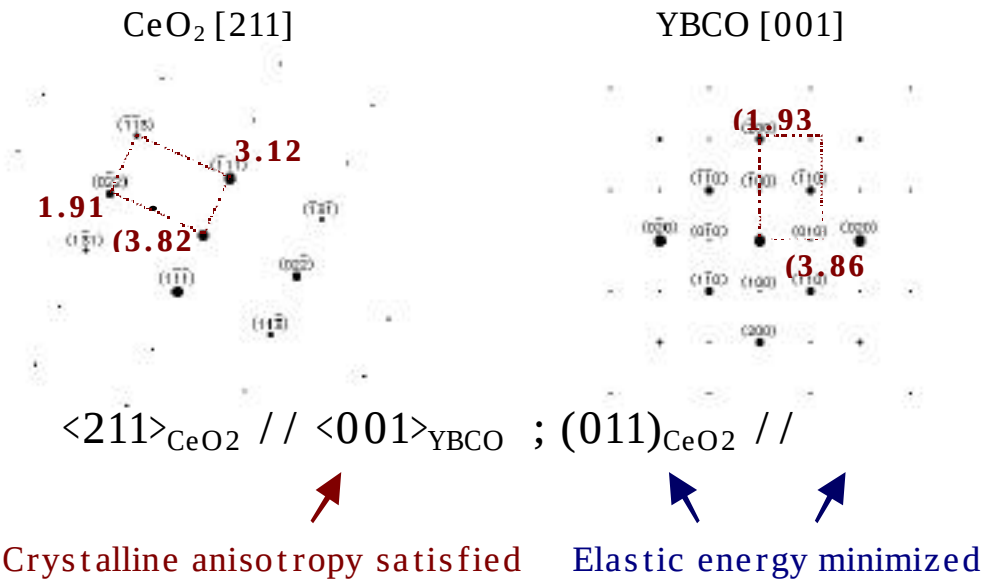

Fig. 15. Reciprocal space representations of CeO_2 [211] and YBCO [001] planes showing that elastic interactions are minimized by orientation relationship CeO_2 (001) // YBCO (010).

Reference:

[1] B. W. Kang, A. Goyal, D. F. Lee, J. E. Mathis, E. D. Specht, P. M. Martin, and D. M. Kroeger, J. Mater. Res. **17**, 1750 (2002).

Interactions

Y. L. Tang, D. J. Miller, R. M. Baurceanu, V. A. Maroni, and R. D. Parella (Am. Superconductor), the authors of "Improved Microstructure in Ag/Bi-2223 Composite Tapes by Systematic Variation of Heat Treatment Parameters", Superconductor Science and Technology, 15, 1365-1371 (2002), were told their article was among the most highly accessed online articles in the journal in 2002.

Balu Balachandran attended the post-peer-review debriefing meeting in Washington, D.C. on Oct. 16, 2002 .

Balu Balachandran visited SuperPower to discuss CRADA activities on Oct. 25, 2002 .

Balu Balachandran attended the 15th International Symposium on Superconductivity in Yokohama, Japan, Nov. 11-13, 2002.

Balu Balachandran visited the National Institute for Materials Science and the Advanced Institute of Science and Technology, Tsukuba on Nov. 14, 2002.

Balu Balachandran visited Sumitomo Electric Industries, Osaka on Nov. 15, 2002.

Balu Balachandran attended the International Superconductivity Industry Summit in Tokyo during Nov. 17-19, 2002.

Vic Maroni organized the symposium "Advances in Superconductivty-Electronics and Electric Power Applications from Atomically Engineered Microstructures" at the Materials Research Society meeting in Boston, MA, Dec. 2-5, 2002.

Beihai Ma and Dean Miller attended the Materials Research Society meeting in Boston, MA, Dec. 2-5, 2002.

Vic Maroni attended the Wire Development Group meeting at American Superconductor Corp. in Westborough, MA on Dec. 6, 2002.

Balu Balachandran attended the CSAC meeting in Washington, DC on Dec. 10, 2002.

Publications and Presentations

Published / Presented

R. M. Baurceanu, V. A. Maroni, N. M. Merchant, A. K. Fischer, M. J. McNallan, and R. D. Parella, Investigation of a Multi-setpoint First Heat Treatment Methodology for the Silver-Sheathed (Bi, Pb)$_2$Sr$_2$Ca$_2$Cu$_3$O$_x$ Composite Conductor, Superconductor Science and Technology, 15, 1167-1175 (2002).

R. M. Baurceanu, V. A. Maroni, N. M. Merchant, A. K. Fischer, M. J. McNallan, and R. D. Parella, Time Evolution of Phase Composition and Microstructure in the Ag/Bi-2223 Composite Superconductor Heat-treated at Specific pO_2/Temperature Setpoints, Superconductor Science and Technology, 15, 1160-1166 (2002).

V. A. Maroni, K. Venkataraman, A. J. Kropf, C. U. Segre, Y. Huang, G. N. Riley, Jr., Nondestructive Analysis of Phase Evolution and Microstructure Development in Ag/(Bi,Pb)$_2$Sr$_2$Ca$_2$Cu$_3$O$_x$ Composite Conductor by 25 keV Transmission X-ray Diffraction, Physica C, 382 , 21-26 (2002).

Y. L. Tang, D. J. Miller, R. M. Baurceanu, V. A. Maroni, and R. D. Parella, Improved Microstructure in Ag/Bi-2223 Composite Tapes by Systematic Variation of Heat Treatment Parameters, Superconductor Science and Technology, 15, 1365-1371 (2002).

J. H. Je (POSTECH), H. You, W. G. Cullen, V. A. Maroni, B. Ma, R. E. Koritala, and C. Thieme (American Superconductor), Detection of a Pd-Ni Interlayer at the Pd/Ni Interface of an Epitaxial Pd Film on Cube Textured Nickel (001), Physica C 383 (2002) 241-246.

U. Balachandran, B. Ma, M. Li, B. L. Fisher, R. E. Koritala, R. Baurceanu, S. E. Dorris, D. J. Miller, K. Venkataraman, and V. A. Maroni, Development of YBCO-Coated Conductors by Inclined-Substrate Deposition, Invited presentation at the Materials Research Society's 2002 Fall Mtg., Boston, Dec. 2-6, 2002.

U. Balachandran, Development of High-Temperature Superconductors for Electric Power Applications, Invited keynote presentation at the XX Mtg. of Physicists of North and Northeast Brazil, Brazilian Physical Society, Recife, Brazil, Nov. 5-8, 2002.

S. Tsukui (Osaka Prefecture U.), R. E. Koritala, M. Li, K. C. Goretta, J. E. Baker (U. of IL at Urbana-Champaign), and J. L. Routbort, Oxygen and Cation Diffusion in YBCO Coated Conductors, Paper presented at the Intl. Symp. on Superconductivity (ISS-2002), Yokohama, Japan, Nov. 11-13, 2002; to be published in Physica C.

U. Balachandran, B. Ma, M. Li, B. L. Fisher, R. E. Koritala, D. E. Miller, and S. E. Dorris, Development of Coated Conductors by Inclined Substrate Deposition, Seminar presented at Sumitomo Electric Industries, Osaka, Japan, Nov. 15, 2002.

U. Balachandran, Development of High-Temperature Superconductors for Electric Power Applications, Seminar presented at National Institute of Advanced Industrial Science and Technology, Tsukuba, Japan, Nov. 14, 2002.

U. Balachandran, B. Ma, M. Li, B. L. Fisher, R. E. Koritala, D. J. Miller, and S. E. Dorris, Development of Coated Conductors by Inclined Substrate Deposition, Invited manuscript presented at the Intl. Symp. on Superconductivity (ISS 2002), Yokohama, Japan, Nov. 11-13, 2002.

Submitted

B. Ma, M. Li, R. E. Koritala, B. L. Fisher, A. R. Markowitz, R. A. Erck, R. Baurceanu, S. E. Dorris, D. J. Miller, and U. Balachandran, Pulsed Laser Deposition of YBCO Films on ISD MgO Buffered Metal Tapes, Submitted to Superconductor Science and Technology (Oct. 2002).

M. Li, B. Ma, R. E. Koritala, B. L. Fisher, K. Venkataraman, V. A. Maroni, V. Blasko-Vlasov, P. Berghuis, U. Welp, K. E. Gray, and U. Balachandran, Pulsed Laser Deposition of c-Axis Untilted YBCO Films on c-Axis Tilted ISD MgO-Buffered Metallic Substrates, Manuscript submitted to Physica C (Oct. 2002).

B. Ma, M. Li, B. L. Fisher, R. E. Koritala, R. M. Baurceanu, S. E. Dorris, and U. Balachandran, Inclined-Substrate Pulsed Laser Deposition of Yttria-Stabilized Zirconia Template Films, Abstract to be presented at the 105th Ann. Mtg. of the American Ceramic Society, Nashville, April 27-30, 2003.

P. S. Shankar and J. P. Singh, Residual Stress Measurements in YBCO-Coated Conductors, Abstract to be presented at the 105th Ann. Mtg. of the American Ceramic Society, Nashville, April 27-30, 2003.

R. M. Baurceanu, S. E. Dorris, T. Wiencek, B. Ma, V. A. Maroni, K. Venkataraman, and U. Balachandran, Copper Additions to Silver Substrates for $YBa_2Cu_3O_{7-\delta}$ Coated Conductors, Abstract to be presented at the 105th Ann. Mtg. of the American Ceramic Society, Nashville, April 27-30, 2003.

Y. X. Zhou, M. Mironova, H. Fang, U. Balachandran, and K. Salama, New Seeding Method for Texturing Y-Ba-Cu-O Bulk Superconductor: Multiple Seeded Melt Growth, Abstract to be presented at the 105th Ann. Mtg. of the American Ceramic Society, Nashville, April 27-30, 2003.

Patents: 2000-2002

Metallic Substrates for High-Temperature Superconductors
T. Truchan, D. Miller, K. C. Goretta, U. Balachandran, and R. Foley (U. of IL)
U.S. Patent No. 6,455,166 (Sept. 24, 2002).

Method for Preparing High Temperature Superconductor
Uthamalingam Balachandran and Michael P. Chudzik
U.S. Patent No. 6,361,598 (March 26, 2002).

Shielded High-T_C BSCCO Tapes or Wires for High-Field Applications
Uthamalingam Balachandran, Milan Lelovic, and Nicholas G. Eror
U.S. Patent No. 6,253,096 (June 26, 2001).

Thermomechanical Means to Improve Critical Current Density of BSCCO Tapes
Uthamalingam Balachandran, Roger B. Poeppel, Pradeep Haldar (IGC), and Lesizek Motowidlo (IGC)
U.S. Patent 6,240,619 (June 5, 2001).

Method of Manufacturing a High Temperature Superconductor with Improved Transport Properties
Uthamalingam Balachandran, Richard Siegel, and Thomas Askew
U.S. Patent No. 6,191,075 (February 20, 2001).

Bearing Design for Flywheel Energy Storage Using High-T_c Superconductors
John R. Hull and Thomas M. Mulcahy
U.S. Patent No. 6,153,958 (Nov. 28, 2000).

Method and Apparatus for Measuring Gravitational Acceleration Utilizing a High Temperature Superconducting Bearing
John R. Hull
U.S. Patent 6,079,267 (June 27, 2000).